

# Adaptive Pulse Coupled Neural Network Parameters for Image Segmentation

Thejaswi H. Raya, Vineetha Bettaiah, and Heggere S. Ranganath

**Abstract**—For over a decade, the Pulse Coupled Neural Network (PCNN) based algorithms have been successfully used in image interpretation applications including image segmentation. There are several versions of the PCNN based image segmentation methods, and the segmentation accuracy of all of them is very sensitive to the values of the network parameters. Most methods treat PCNN parameters like linking coefficient and primary firing threshold as global parameters, and determine them by trial-and-error. The automatic determination of appropriate values for linking coefficient, and primary firing threshold is a challenging problem and deserves further research. This paper presents a method for obtaining global as well as local values for the linking coefficient and the primary firing threshold for neurons directly from the image statistics. Extensive simulation results show that the proposed approach achieves excellent segmentation accuracy comparable to the best accuracy obtainable by trial-and-error for a variety of images.

**Keywords**—Automatic Selection of PCNN Parameters, Image Segmentation, Neural Networks, Pulse Coupled Neural Network

## 1. INTRODUCTION

THE single layered Pulse Coupled Neural Network (PCNN) is a laterally connected two-dimensional array of artificial neurons known as Pulse Coupled Neurons (PCN). Though Eckhorn did not refer to his neuron model as PCN, the artificial neuron model (Eckhorn's neuron) developed by him based on the study of the visual cortex of cats is the first PCN model [1]. By using a laterally connected recurrent network of Eckhorn's neurons, he was successful in emulating some of the neuro-physiological phenomena observed in cat's visual cortex. Ranganath, Kuntimad and Johnson modified Eckhorn's model for image processing applications including image segmentation, smoothing and object detection. They called the simplified model the pulse coupled neuron [2]. Both neuron models are being used for image segmentation.

Though there are several PCNN based image segmentation methods, even today, the single-burst algorithm developed by Kuntimad and Ranganath in 1999 is considered a classic algorithm [3]-[4]. The segmentation accuracy of the single-burst PCNN algorithm has been compared with those of other widely used segmentation methods by segmenting several images consisting of two regions, object and background, in

which intensity ranges of object and background regions overlap significantly. The segmentation result of the PCNN based algorithm was found to be consistently better than the segmentation results obtained by optimal thresholding, region growing, split-and merge, and probabilistic relaxation algorithms [3]. It has been proved that the single-burst PCNN can segment a two-region image perfectly even if the two intensity ranges overlap significantly when there exist linking coefficient and linking radius values for which two inequalities involving linking coefficient, linking radius, object pixel intensity range, and background pixel intensity range are consistent [4]. However, no method has been suggested for the automatic determination of the two parameters from image statistics. Karvonen used the PCNN to segment Baltic sea ice Synthetic Aperture Radar (SAR) images [5]. He estimated the Gaussian probability density function that best represented the histogram of each region, and calculated the primary firing threshold and the linking coefficient for each region. Though his approach may have suited to segment Baltic ice SAR images it is not expected to give satisfactory result when region pixel intensity distribution can not be approximated by a Gaussian probability density function. In many cases, the image or region histogram may not even be bi-modal. Therefore, automatic determination of primary firing thresholds and the corresponding linking coefficient values is still an open problem. The PCNN based image segmentation process can be viewed as a region growing method where seed pixels are identified by the neurons that fire during primary firing, and the region growing is accomplished by capturing spatially connected neighboring neurons through secondary firing. Stewart et. al. have used PCNN to develop a seeded region growing method in which seed locations are internally generated [6]. They have avoided the difficulty of choosing optimal value for the linking coefficient for each region by gradually incrementing the value of the linking coefficient to grow the region in multiple steps. The process terminates when at least one of the three termination conditions they have specified is satisfied.

A few researchers have used the PCNN with the original Eckhorn's neuron model to segment images [7]-[9]. Note that Eckhorn's neuron consists of a feeding receptive field, a linking receptive field, and a spike or pulse generator. The spike generator has one leaky integrator, the output of which is the threshold signal. The feeding and linking receptive fields have several leaky integrators. Each leaky integrator has two parameters, amplitude and decay time constant. Even if we assume that all leaky integrators in each receptive field

T. H. Raya is with the University of Alabama in Huntsville, Huntsville, AL 35899 USA (phone: 678-979-6907; fax: 256-824-6239; e-mail: thr0001@cs.uah.edu).

V. Bettaiah is with the University of Alabama in Huntsville, Huntsville, AL 35899 USA (e-mail: vb0003@cs.uah.edu).

H. S. Ranganath is with the University of Alabama in Huntsville, Huntsville, AL 35899 USA (phone: 256-824-6653; e-mail: ranganat@cs.uah.edu).

are identical, there are six parameters. The linking coefficient is the seventh parameter. It is obvious that selection of appropriate values for these parameters is a challenging problem. Usually these parameter values are determined by trial-and-error. Also, when Eckhorn's model is used a neuron is allowed to pulse more than once during the segmentation process. Ma *et al.* have allowed the pulsing activity to continue for a large number of iterations (a few thousand). At the end of every iteration, the entropy of the segmented image is computed. The segmented image of the iteration at which the entropy attains its maximum value is taken as the final result. Based on the experiments conducted, they claim that as entropy increases the details in the segmented image increase [7]. Ma, Liu, and Qian have also suggested that a possible way for automating the selection of the segmentation result is by selecting the result of the iteration for which the discrepancy between the input image and the segmented image as measured by the cross-entropy is minimum [8].

As the accuracy of a PCNN based image segmentation algorithm is very sensitive and depends on the values of the PCNN parameters, it is important to develop a method for the automatic determination of appropriate values for all PCNN parameters based on image statistics. This paper presents a method for computing the linking coefficient and the primary firing threshold directly from the image histogram. The approach can be used to obtain global as well as adaptive local values for both parameters.

The PCNN based single-burst image segmentation algorithm is briefly described in Section II. An analysis of the single-burst segmentation algorithm and the role played by the linking coefficient and the primary firing threshold are given in Section III. Two methods for the determination of values for the linking coefficient and primary firing threshold are given in Sections IV and V. Section VI presents simulation results. Finally, discussion and conclusions are given in Section VII.

## II. PCNN BASED SINGLE-BURST IMAGE SEGMENTATION ALGORITHM

This section briefly describes the  $N \times N$  laterally connected single-layer PCNN operating in single-burst mode that was developed by Kuntimad and Ranganath to segment an  $N \times N$  image [3]-[4]. There is one-to-one correspondence between image pixels and PCNN neurons. The neuron  $N_{i,j}$  corresponding to pixel  $(i, j)$  consists of a feeding input  $X_{i,j}$  (intensity of image pixel  $(i, j)$ ), a linking receptive field which gathers linking input  $L_{i,j}(t)$  from its 8-neighbors, and a pulse generator as shown in Fig. 1. The internal activity of  $N_{i,j}$  is computed by combining the feeding and linking inputs as

$$U_{i,j}(t) = X_{i,j}(1 + \beta L_{i,j}(t)) \quad (1)$$

where,  $\beta > 0$  is a global parameter known as the linking coefficient. When  $U_{i,j}(t) > \theta_{i,j}(t)$ , the neuron  $N_{i,j}$  fires ( $Y_{i,j}(t) = 1$ ) and sends linking input to each of its 8-neighbors through a linking leaky integrator (LLI), and also charges the threshold signal generator to a very high value  $\theta_{max}$  to ensure that  $N_{i,j}$  will not fire again in the current pulsing cycle [3]. All leaky integrators are considered identical with an impulse response of  $V e^{-t/\tau}$  where  $V$  is the amplitude and  $\tau$  is the decay

time constant. One may prefer to use unit linking and avoid the use of leaky integrators in the linking receptive field.

Consider an image of two regions, object and background. Assume that the object is brighter than the background. Let  $(Bmin, Bmax)$  and  $(Omin, Omax)$  be intensity ranges of the background and object pixels. If  $Bmax > Omin$  then the two intensity ranges overlap, and perfect segmentation becomes difficult to achieve. In fact, the number of pixels incorrectly assigned increases as the extent of the overlap increases.

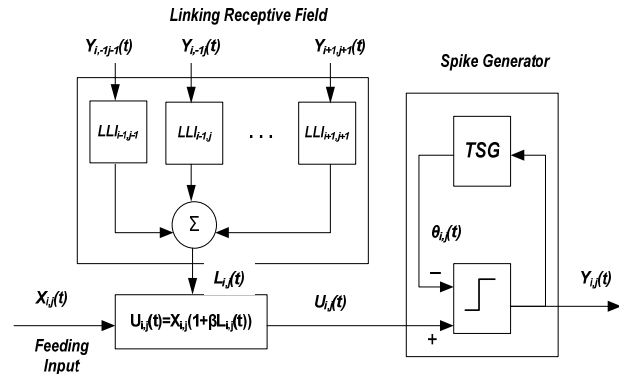


Fig. 1 The Pulse Coupled Neuron Model

However, it has been shown that PCNN segments such images perfectly if the following two inequalities are satisfied [4].

- 1) The neurons corresponding to the object pixels with intensity  $Omax$  pulse naturally (primary pulsing without the help of linking input) at time  $t = T(Omax)$  where  $T(Omax)$  is the time required for the threshold signals to decay from their maximum value of  $\theta_{max}$  to  $Omax$ .
- 2) During secondary firing due to fast linking, all object neurons for which the following inequality is true are captured.

$$X_{i,j}(1 + \beta L_{i,j}(T(Omax))) \geq Omax \quad (2)$$

In the above inequality,  $\beta$  is the linking coefficient,  $L_{i,j}(T(Omax))$  is the total linking input received by  $N_{i,j}$  from its 8-neighbors, and  $X_{i,j}$  is the intensity of pixel  $(i, j)$ .

- 3) Similarly, during secondary firing, all background neurons for which the following inequality is not true are also captured.

$$X_{p,q}(1 + \beta L_{p,q}(T(Omax))) < Omax \quad (3)$$

If it is possible to find a value of  $\beta$  for which the inequality (2) is true for all object neurons and the inequality (3) is true for all background neurons, then only the object neurons can be made to pulse together at  $T(Omax)$  and thus leading to perfect segmentation of the input. When perfect segmentation is not possible the goal is to capture maximum number of object neurons and minimum number of background neurons as possible.

### III. ANALYSIS OF PCNN BASED IMAGE SEGMENTATION ALGORITHM

It is obvious that inequalities (2) and (3) impose opposing conditions on  $\beta$ . Inequality (2) specifies the lower bound ( $\beta_l$ ), and inequality (3) specifies the upper bound ( $\beta_u$ ) for  $\beta$ . The value of  $\beta_l$  increases as the intensity ratio  $Omax/Omin$  increases, and the value of  $\beta_u$  decreases as the ratio  $Omax/Bmax$  decreases. Any image for which  $\beta_l > \beta_u$  perfect segmentation is not possible. Preprocessing the input image or enhancing the neuron model that effectively reduces  $\beta_l$  and increases  $\beta_u$  improves segmentation accuracy. Smoothing the image compresses the dynamic range of each region and also reduces the extent of intensity range overlap of regions. The net effect is a reduction in the value of  $\beta_l$  and an increase in the value of  $\beta_u$  as desired [3]. Kuntimad achieved improvement in segmentation accuracy by delaying the primary firing to a value below  $Omax$ . This was accomplished by allowing the inactive neurons in the linking receptive field to send inhibitory linking inputs [4]. The approach is not biologically plausible, and also may not always improve segmentation. Note that delaying the primary firing to a value below  $Omax$  decreases values of both  $\beta_l$  and  $\beta_u$ . This is beneficial only if the benefit of the reduction in the value of  $\beta_l$  is relatively more than the harm caused by the reduction in the value of  $\beta_u$ . Also, he has not addressed the problem of determining the value of the threshold or intensity at which primary firing must begin.

Therefore, associated with the above approach, there are three major problems or issues which should be solved to further improve the segmentation accuracy of the PCNN approach.

- 1) The accuracy of the PCNN based algorithms is very sensitive to the values assigned to linking coefficient and linking neighborhood radius. Almost always the linking radius is fixed at 1.5. Each neuron receives linking input from its 8-neighbours. Previous experience with PCNN shows that a small change in the value of  $\beta$  changes the segmentation result significantly. Therefore, it is important to develop a quantitative approach to determine a suitable value of  $\beta$  rather than determine its value by trial-and-error approach. To the best of our knowledge the determination of the optimal or near optimal value for the linking coefficient  $\beta$  directly from the image is still an open problem that needs to be solved.
- 2) It is very beneficial if one can delay primary firing to an appropriate intensity level between  $Omax$  and  $Bmax$ , say  $PFT$ . This effectively reduces the lower bound for  $\beta$  which is desirable. Also, prevents stray bright pixels from triggering primary firing leading to unacceptable segmentation result. At the same time,  $PFT$  must be large enough to prevent brighter background neurons from firing with object neurons in large numbers. Therefore, there is a need to develop a method to determine an appropriate value for the primary firing threshold  $PFT$  from the image itself.
- 3) Because of non-uniform illumination, varying object-background intensity contrast or differing noise levels, it

may not be practical to use global values for  $PFT$  and  $\beta$ . In other words, it is desirable to make both parameters local and assign values based on local image intensity attributes. In the limiting case, each neuron can have its own parameter values. A good compromise is to partition the image into subimages and assign appropriate parameter values to each subimage.

### IV. GLOBAL LINKING COEFFICIENT AND PRIMARY FIRING THRESHOLD

Now consider the segmentation of an image with two regions, object and background. Assume that intensity ranges of object pixels and background pixels overlap considerably. The goal is to find near optimal values for  $PFT$  and  $\beta$  so that the PCNN produces good segmentation result. The method for computing global  $PFT$  and  $\beta$  directly from the image statistics is described below.

- 1) For the image to be segmented, threshold  $T$  which roughly segments the image into two regions (object and background) is determined. The threshold  $T$  may be obtained using the basic iterative method, Otsu's method which maximizes inter-class variance or by locating the valley of the histogram if the histogram is bimodal. The intensity mean  $m_O$  and standard deviation  $\sigma_O$  of object pixels are approximated using image pixels with intensity greater than  $T$ . Similarly, the intensity mean  $m_B$  and standard deviation  $\sigma_B$  of background pixels are approximated using image pixels with intensity less than or equal to  $T$ .
- 2) The primary firing threshold  $PFT$  should be greater than  $T$  to prevent bright noisy background pixels from firing during the primary firing. Thus,  $PFT$  is computed as
- 3) The linking coefficients  $\beta$  should be computed such that the following inequality is true for all object neurons.

$$PFT = (m_O + k_l \sigma_O) \quad (4)$$

where,  $k$  is a constant greater than zero. Typically,  $k_l$  is in the range [1, 2].

$$Omin (1 + \beta LI(t)) \geq PFT \quad (5)$$

The minimum object intensity  $Omin$  is not known and is roughly taken as  $(T - k_2 \sigma_O)$ . It is reasonable to expect more object neurons than background neurons in the 8-neighborhood of an object neuron. Therefore, assuming unity linking, the minimum value of  $LI(t)$  for an object neuron may be taken as 5. Therefore, the linking coefficient  $\beta$  is computed as

$$\beta = (PFT / (T - k_2 \sigma_O) - 1) / 5 \quad (6)$$

Usually,  $k_2$  is a positive number in the range [0.5, 1.0].

### V. ADAPTIVE LINKING COEFFICIENTS AND PRIMARY FIRING THRESHOLDS

Often, it is not practical to use a global value for the linking coefficient or the primary firing threshold. This could happen due to a variety of reasons such as non-uniform illumination, varying contrast between object and background regions, and noise characteristics as described below.

- 1) Consider two areas of object (background) whose intensities would approximately be the same under uniform illumination. If the illumination is not uniform

then object (background) pixels in the area where illumination is relatively higher will be significantly brighter than the object (background) pixels in the area where illumination is lower. Non-uniform illumination, in general, expands the object and background intensity ranges.

- 2) The contrast between object and background pixels as measured by intensity difference also changes as illumination changes. Thus, the non-uniform illumination increases the extent by which object and background intensity ranges overlap.
- 3) The standard deviation of pixel intensity may not be uniform throughout the image due to shadows (non-uniform illumination) and varying noise characteristics.

As a result, values of parameters suitable for one part of the image may not be suitable for other parts. In such cases, it is necessary to adapt parameter values to match the local image properties. As an extreme case, one may wish to compute values of  $\beta$  and  $PFT$  for each neuron. The development of an approach to accomplish this task is challenging and has not been done so far. In this section, two methods for computing  $\beta$  and  $PFT$  for individual neurons are described. The first method consists of the following steps.

- 1) The image to be segmented is partitioned into  $(K \times L)$  non-overlapping subimages or blocks.
- 2) The global values of the linking coefficient and the primary firing threshold are computed for each block as described in Section IV. Let  $\beta_G[i, j]$  and  $PFT_G[i, j]$  be the linking coefficient and the primary firing threshold for the block  $BLK[i, j]$ .
- 3) If necessary, the possibility of abrupt change of parameter values between adjacent blocks is avoided by using interpolation in two steps. For example, consider the computation of the primary firing threshold for neurons in  $BLK[i, j]$ . In the first step, for all neurons in  $D$  columns on either side of the boundary between adjacent blocks  $BLK[i, j-1]$  and  $BLK[i, j]$ , the primary firing threshold is modified to change linearly along the rows from  $PFT_G[i, j-1]$  to  $PFT_G[i, j]$ . In the second step, for all neurons in  $D$  rows on either side of the boundary between blocks  $BLK[i-1, j]$  and  $BLK[i, j]$  the primary firing threshold is further modified to change linearly along the columns from the modified value in  $BLK[i-1, j]$  to the modified value in  $BLK[i, j]$ . A similar process is used to assign linking coefficient values to individual neurons.

The second method consists of the following steps.

- 1) The image to be segmented is divided into  $(K \times K)$  overlapping subimages or blocks. For adjacent blocks  $BLK[i-1, j]$  and  $BLK[i, j]$ , the bottom 50% of the rows in  $BLK[i-1, j]$  are same as the top 50% of the rows in  $BLK[i, j]$ . Similarly, for adjacent blocks  $BLK[i, j]$  and  $BLK[i, j+1]$ , the right 50% of the columns in  $BLK[i, j]$  are same as the left 50% of the columns in  $BLK[i, j+1]$ .
- 2) The global values of the linking coefficient and the primary firing threshold are computed for each block as described in Section III. Let  $\beta_G[i, j]$  and  $PFT_G[i, j]$

be the linking coefficient and the primary firing threshold for the block  $BLK[i, j]$ .

- 3) Because of the overlapping partitioning, a neuron belongs to 1, 2 or 4 blocks depending on its location in the PCNN. Most neurons belong to 4 blocks. Therefore, the parameter value for a neuron is computed as the weighted sum of values of all blocks to which the neuron belongs. The value of each weight is in the range  $[0, 1]$  and the sum of all weights associated with a neuron is 1. The value of the weight that multiplies the global parameter of a block is inversely proportional to the distance of the neuron from the center of the block.

## VI. SIMULATION RESULTS

This section presents simulation results that validate the concepts and algorithms described in detail in the previous sections.

*A. The PCNN based image segmentation algorithm is able to segment an image perfectly even when object and background intensity ranges overlap significantly if inequalities (2) and (3) are true.*

Fig. 2 (a) shows a two-region image for which  $Omin = 120$ ,  $Omax = 200$ ,  $Bmin = 40$ , and  $Bmax = 140$ . When this image is applied as input to the PCNN for segmentation, all neurons corresponding to pixels with intensity 200 fire first (primary firing), and then initiate secondary firing. Inequality (2) establishes the lower limit for the value of  $\beta$ . The value of  $\beta$  must be large enough to capture object neurons corresponding to pixels of intensity 120 even when the linking inputs received by them are at their minimum values. Therefore,

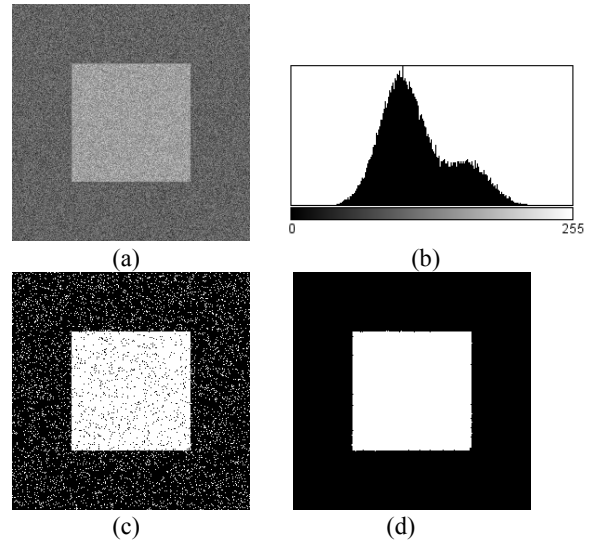


Fig. 2 Illustration of perfect image segmentation using PCNN. (a) Two-region image with additive

Gaussian noise with mean 0 and standard deviation 20. (b) Image histogram. (c) Result of segmenting the image in (a) using Otsu's optimal thresholding method. (d) Result of segmenting the image in

(a) using PCNN.

assuming that all object neurons get linking input from at least 5 out of 8 neighbors, the lower limit for  $\beta$  is  $(200/120 - 1) / 5 = 2/15$ . The value of  $\beta$  must be small enough to not to capture background neurons corresponding to pixels of intensity 140 even when the linking inputs received by them from neighboring object neuron are at their maximum values. Inequality (3) establishes the upper limit for the value of  $\beta$ . Therefore, assuming that all background neurons get linking input from at most 3 out of 8 neighbors, the upper limit for  $\beta$  is  $(200/140 - 1) / 3 = 1/7$ . As the upper limit is greater than the lower limit, the PCNN gives perfect result if  $PFT = 200$  and  $1/7 > \beta > 2/15$ . The segmentation result obtained with  $PFT = 200$  and  $\beta = 0.14$  is shown in Fig. 2 (d). For comparison purpose, segmentation result obtained from Otsu's optimal thresholding method is shown in Fig. 2 (c).

*B. If one or two of inequalities (2) and (3) are not true then perfect segmentation is not possible. However, the accuracy of the PCNN based image segmentation algorithm can be greatly improved by delaying the primary firing threshold (PFT) to an appropriate value between  $B_{max}$  and  $O_{max}$ .*

The image in Fig 3 (a) is similar to the image in Fig. 2 (a) in content. However, contrast between object and background is poor and the noise level is high (Standard Deviation = 40). For the image in Fig. 3(a),  $O_{min} = 20$ ,  $O_{max} = 200$ ,  $B_{min} = 1$ , and  $B_{max} = 80$ . It is not possible to find a value of  $\beta$  for which inequalities (2) and (3) are both true, and therefore

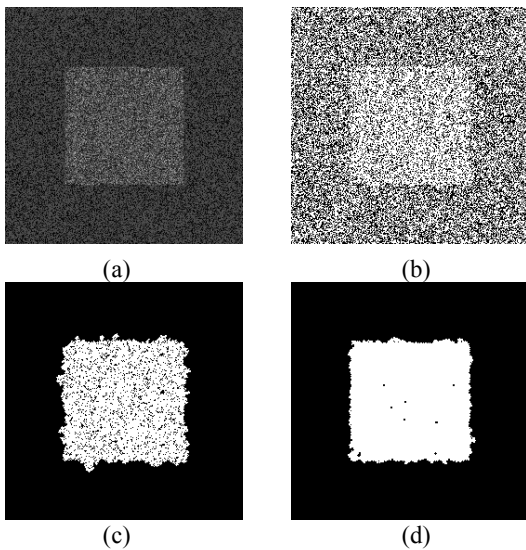


Fig. 3 Effect of delaying the primary firing threshold on segmentation accuracy. (a) Two-region image with additive Gaussian noise of mean 0 and standard deviation 40. (b) Result of segmenting the image in (a) using Otsu's optimal thresholding method. (c) Result of segmenting the image in (a) using PCNN with  $O_{max} = 200$  as the primary firing threshold. (d) Result of segmenting the image in (a) using PCNN with  $PFT = 190$  as the primary firing threshold.

perfect segmentation is not achievable. As there is significant overlap between object and background intensity ranges, this

is not an easy image to segment. This is illustrated by the poor quality of the segmentation result obtained by Otsu's optimal thresholding algorithm shown in Fig 3 (b). Even under these adverse conditions, the PCNN gives remarkably better result compared to Otsu's method as shown in Fig 3 (c). The value of  $\beta$  was varied by trial-and-error to obtain the best result (judged by visual inspection). In Section III, it is stated that it is possible to obtain significantly better results by delaying the primary firing to an appropriate intensity level ( $PFT$ ) less than  $O_{max}$ . The result in Fig 3 (d) is obtained by setting  $PFT$  to 190. Once again the value of  $\beta$  is obtained by trial-and-error.

*C. If the intensity characteristics of an image vary significantly across the image then improved segmentation result may be obtained by using adaptive local parameters instead of using a single set of global parameters.*

The image in Fig 4 (a) is obtained by modifying the image in Fig 2(a) to achieve the effect of non-uniform illumination. The illumination of the image in Fig. 4 (a) increases linearly from left to right. Note the difference in the histograms in Fig 2 (b) and Fig. 4 (b). The image has changed for worse as far segmentation is concerned. As  $O_{min} = 84$ ,  $O_{max} = 214$ ,  $B_{min} = 20$ , and  $B_{max} = 177$ , it is not possible to find a value of  $\beta$  for which inequalities (2) and (3) are both true, and therefore perfect segmentation is not achievable for all values of the primary firing threshold. However, the PCNN produces better result than most other methods if  $\beta$  and  $PFT$  are set to proper values. The result in Fig 4 (c) is obtained by setting  $\beta$  and  $PFT$  to 0.30 and 200, respectively. These values are obtained by trial-and-error. In order to illustrate that the use of adaptive parameters improves segmentation accuracy, the image in Fig 4 (a) is split into two blocks of size  $256 \times 128$

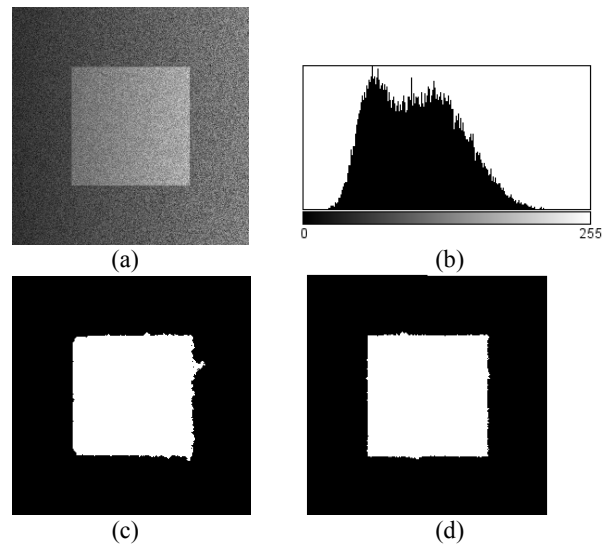


Fig. 4 Illustration of segmentation of an image with non-uniform illumination using PCNN.

(a) Two-region image with linearly increasing illumination from left to right, and additive Gaussian noise of mean 0 and standard deviation 20. (b) Image histogram. (c) Result of segmenting the image in (a) using PCNN with  $PFT = 200$  and  $\beta = 0.30$ . (d) Result of segmenting the image in (a) using PCNN with adaptive parameters. (vertically at the center) and each block is segmented independently. The values of  $\beta$  and  $PFT$  for the left block are 0.28 and 165, respectively. The values of  $\beta$  and  $PFT$  for the right block are 0.26 and 210, respectively. The improved segmentation result obtained by using adaptive parameters is shown in Fig. 4 (d).

*D. The values of  $\beta$  and  $PFT$  obtained using the methods proposed in Sections IV and V are able to produce near optimal segmentation results.*

Now consider the segmentation of the three images in Fig. 2 (a), Fig. 3 (a), Fig. 4 (a) using the parameters values computed as described by the methods given in Sections IV and V. The threshold  $T$  that roughly partitions the image in Fig. 2 (a) into object and background regions is computed using Otsu's method and its value is 126. The object's mean intensity  $m_O$  and standard deviation  $\sigma_O$ , approximated by the mean and standard deviation of all pixels with intensity greater than  $T$ , are 154.5 and 19.62, respectively. Then,  $PFT$  (194) and  $\beta$  (0.17) are computed as  $(m_O + 2\sigma_O)$  and  $0.2 * [PFT / (T - \sigma_O) - 1]$ , respectively. The segmentation result obtained using these values is shown in Fig. 5 (a).

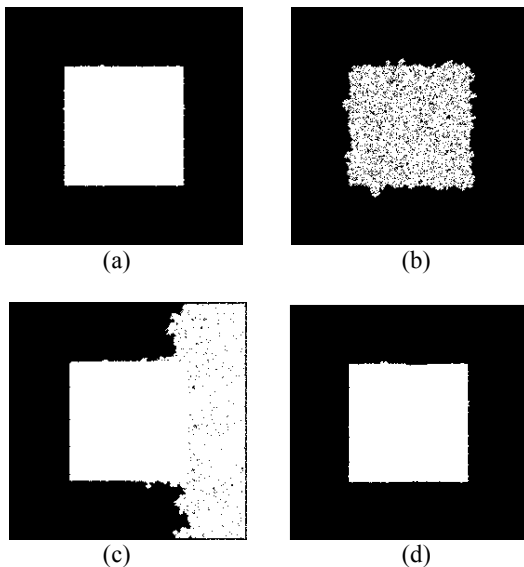


Fig. 5 Segmentation results using adaptive values of  $PFT$  and  $\beta$  calculated using the methods proposed in Sections IV and V. (a) Result of segmenting the image in Fig. 2 (a) using global  $PFT$  and  $\beta$ . (b) Result of segmenting the image in Fig. 3 (a) using global  $PFT$  and  $\beta$ . (c) Result of segmenting the image in Fig. 4 (a) using global  $PFT$  and  $\beta$ . (d) Result of segmenting the image in Fig. 4 (a) using adaptive  $PFT$  and  $\beta$ .

Otsu's threshold, object's mean intensity and standard deviation for the image in Fig. 3 (a) are 55, 81 and 20, respectively. Therefore,  $PFT$  is 121 and  $\beta$  is 0.37. The result of segmenting the image in 3 (a) is displayed in Fig. 5 (b). A

comparison of segmented images in Fig 5 (a) and Fig. 5 (b) with the images in Fig. 2 (d) and Fig. 3 (d) shows that the use of automated parameter values has produced segmentation results very similar to the best results obtained by trial-and-error approach in both cases.

When the image in 4 (a) is segmented using global  $PFT$  and  $\beta$ , the segmentation result obtained is not comparable to the result in Fig. 4 (c). However, when the image is partitioned into two blocks vertically at the center and each block is independently segmented almost perfect segmentation is achieved. Otsu's threshold, object mean, standard deviation,  $PFT$  and  $\beta$  for the left block are 92, 121, 18, 160 and 0.23, respectively. For the right block these numbers are 124, 149, 19, 187 and 0.14. The segmented image, shown in Fig. 5 (d), is comparable to the image in Fig. 4 (d) in quality.

*E. In general, the segmentation accuracy is less sensitive to the variation in the value of  $k_1$  than it is to the variation in the value of  $\beta$ .*

The image in 2 (a) is segmented by varying the value of  $k_1$  from 1 to 2 in steps of 0.1. No noticeable difference is found in the final results obtained. Several other images are then segmented by varying  $k_1$ . In all cases, simulation results indicate that the segmentation accuracy remains fairly insensitive to the value of  $k$  in the range [1, 2]. This is perhaps due to the fact that the values of  $PFT$  and  $\beta$  both increase or decrease together as  $k_1$  is increased or decreased, respectively.

*F. If an image is highly noisy, in general, the segmentation accuracy can be improved by smoothing the image before segmentation.*

Fig. 6 (a) shows an image obtained with non-uniform illumination. The illumination increases linearly from left to right. The image is also corrupted with additive Gaussian noise (mean = 0 and standard deviation = 20). It is obvious from the histogram that this is a difficult image to segment using any region thresholding method. The image is

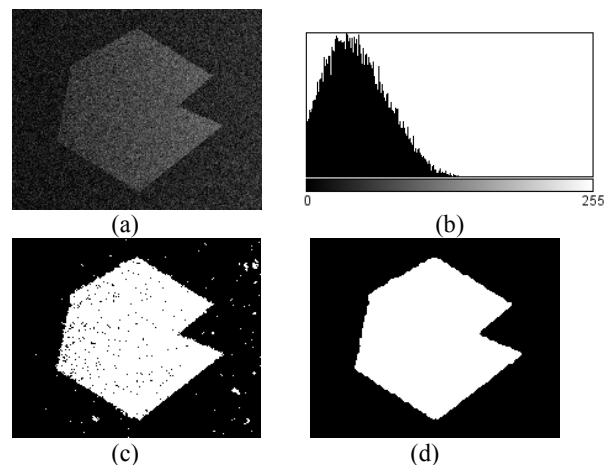


Fig. 6 Effect of smoothing on the performance of PCNN.

(a) Noisy image obtained under non-uniform illumination. (b) Image histogram. (c) Segmentation result without smoothing. (d) Segmentation result with smoothing (Original image taken from Digital Image Processing, 3rd Edition, Rafael C. Gonzalez and Richard E. Woods).

partitioned into  $(2 \times 2)$  non-overlapping blocks (each block is a  $150 \times 200$  subimage) and segmented by calculating  $PFT$  and  $\beta$  for each block as described in Section IV. Because of relatively high noise several pixels were misclassified by the PCNN as shown in Fig. 6 (c). Of course, the result is much better than what can be obtained by an optimal thresholding method. However, when smoothed image is applied as input the PCNN produced almost perfect segmentation result as shown in Fig. 6 (d).

*G. If block approach is used for computing adaptive PFT and  $\beta$  then interpolation becomes a necessity when the value of a parameter changes significantly from one block to another.*

The yeast image in Fig. 7 (a) is partitioned into  $(4 \times 4)$  blocks for the computation of adaptive parameters. There is a significant difference between the values of  $PFT$  for the third and fourth blocks (59 and 35) in the first row. If Interpolation is not used to make  $PFT$  change gradually from  $BLK [1, 3]$  to  $BLK [1, 4]$  then undesirable block effects appear in the segmented image. Even after interpolation slight block effect can be seen in the top right corner of the segmented image in Fig. 7 (b).

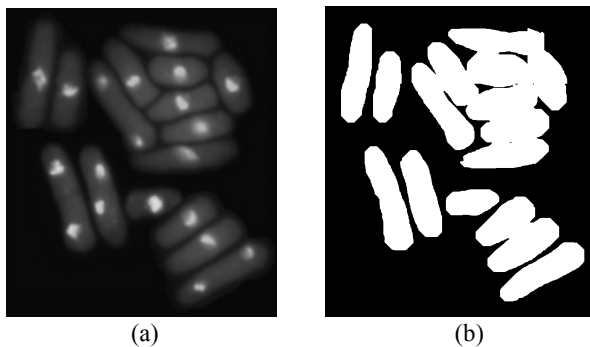


Fig. 7 Illustration of block effect. (a) Input image. (b) Result of segmenting the image in (a) using PCNN (Original image courtesy of Professor Susan L. Forsburg, University of Southern California).

## VII. CONCLUSION

The pulse coupled neural network operating in single-burst mode is capable of segmenting two-region images accurately under very adverse conditions as long as the linking coefficient and the primary firing threshold are set to appropriate values. For years, the task of automatic computation of optimal or near optimal values for these two critical parameters has remained an elusive goal. The major contribution of this paper is a quantitative approach for the automatic computation of the linking coefficient and the primary firing threshold directly from the image histogram. It has been shown that the approach can be used for computing one set of global parameters for the entire image, or adaptive local parameters for each neuron without compromising image

segmentation quality or accuracy. Extensive simulation shows that the segmentation accuracy attained by using the automatically computed global parameters is comparable to the best results achieved by setting the parameter values by trial-and-error. When an image requires adaptive local parameters, it is almost impossible to use trial-and-error approach. On the contrary, the proposed approach partitions the image into overlapping or non-overlapping subimages or blocks, and computes the parameters for each subimage. Interpolation may be used to determine parameter values for individual neurons.

For all images segmented object mean intensity plus twice the object intensity standard deviation is found to be a good value for the primary firing threshold. The value of the linking coefficient obtained by estimating the minimum object pixel intensity as Otsu's threshold minus object intensity standard deviation has given good results. Background intensity mean and standard deviations are not at all used. Future research should focus on using these values in estimating  $PFT$  and  $\beta$ . One possibility is to compute  $PFT$  and  $\beta$  for the image and its inverted image and use the average values for segmenting the image.

It is desirable to have the ability to determine automatically if the global parameters are sufficient or not to segment an image. When there is a need to use adaptive local parameters, it should be possible to determine the number of blocks into which the image must be partitioned. Future work should focus on automating the partitioning of the image to be segmented.

## REFERENCES

- [1] R. Eckhorn, H.J. Reitboeck, M. Arndt, and P.W. Dicke, "Feature linking vis synchronization among distributed assemblies: Simulation results from cat visual cortex and from simulations," in *Neural comput.*, Vol 2, pp.293-307, 1990.
- [2] H. S. Ranganath, G. Kuntimad, and J. L. Johnson, "pulse coupled neural networks for image processing," *IEEE Southeastcon*, Raleigh, NC, Mar. 1995.
- [3] G. Kuntimad, "Pulse coupled neural networks for image processing," Ph.D. dissertation, Department of Computer Science, The University of Alabama in Huntsville, 1995.
- [4] G. Kuntimad and H.S. Ranganath, "Perfect segmentation using pulse coupled neural networks," *IEEE Transactions on Neural networks*, Vol. 10, No. 3, pp. 591-598, 1999.
- [5] J. A. Karvonen, "Baltic sea ice SAR segmentation and classification using modified pulse coupled neural networks," *IEEE Transactions on Geoscience and Remote Sensing*, Vol 42, No. 7, pp. 1566-1574, 2004.
- [6] R. D. Stewart, I. Fermin, and M. Opper, "Region growing with pulse coupled neural networks: an alternative to seeded region growing," *IEEE Transactions on Neural Networks*, Vol. 13, No. 6, pp.1557-1562, 2002.
- [7] Y. Ma, R. Dai, and L. Li, "Image segmentation of embryonic plant cell using pulse coupled neural networks," *Chinese Science Bulletin*, Vol. 47, No. 2, pp. 167-172, 2002.
- [8] Y. Ma, Q. Liu, and Z. Quian, "Automated image segmentation using improved PCN model based on cross-entropy," *Journal of Image and Graphics*, Vol. 10, pp. 579-584, 2005.
- [9] Xiao, Shi, and Chang, "Automatic image segmentation based on PCNN and fuzzy mutual information," *IEEE Ninth International Conference on Computer and Information Technology*, pp. 241-245, 2009.